

Electronic Supplementary Information

Polypyrrole coated UCNPs@mSiO₂@ZnO nanocomposite for combined photodynamic and photothermal therapy

Qi Cai,^a Jiating Xu,^a Dan Yang,^a Yunlu Dai,^a Guixin Yang,^a Chongna Zhong,^a Shili
Gai,^{*a} Fei He,^a and Piaoping Yang^{*ab}

^a Key Laboratory of Superlight Materials and Surface Technology, Ministry of Education, Harbin
Engineering University, Harbin 150001, P. R. China

^b College of Sciences, Heihe University, 164300, P. R. China

*Email - yangpiaoping@hrbeu.edu.cn

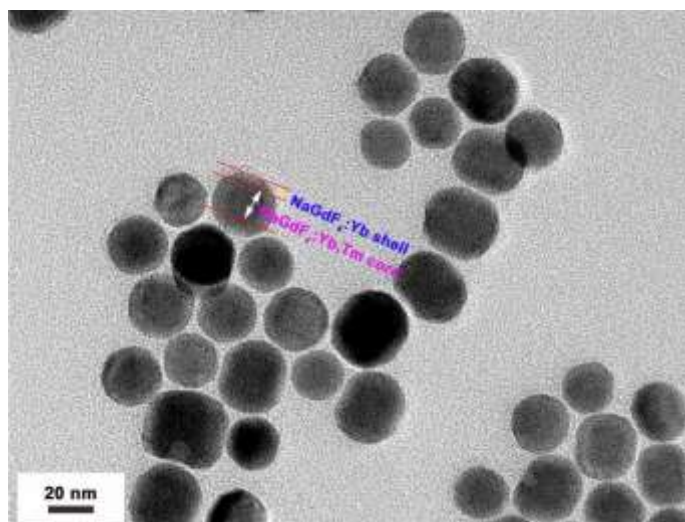


Fig. S1 TEM image of $\text{NaGdF}_4\text{:Yb,Tm@NaGdF}_4\text{:Yb}$ core-shell nanoparticles.

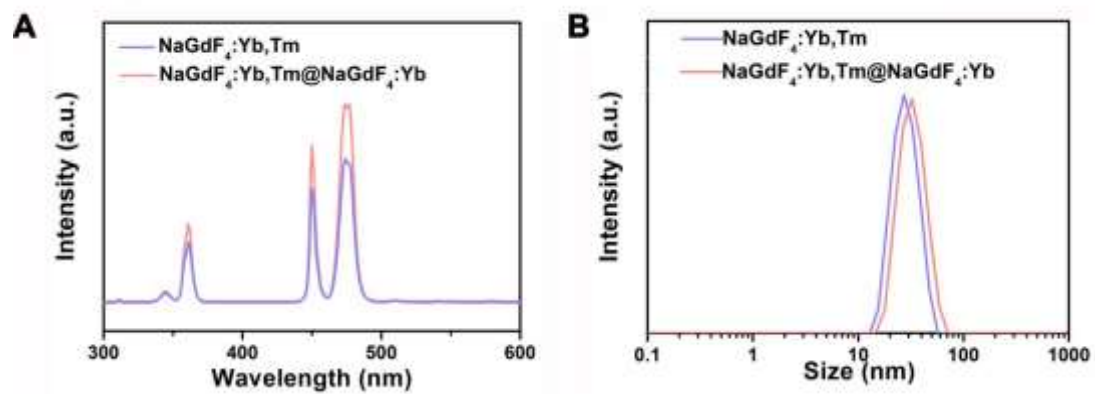


Fig. S2 (A) Upconversion emission spectra and (B) DLS of NaGdF₄:Yb,Tm core and NaGdF₄:Yb,Tm@NaGdF₄:Yb core-shell nanoparticles.

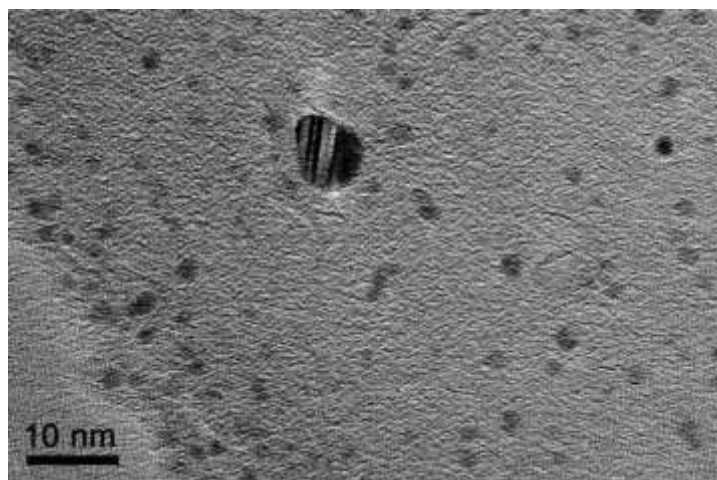


Fig. S3 TEM image of ZnO nanodots.

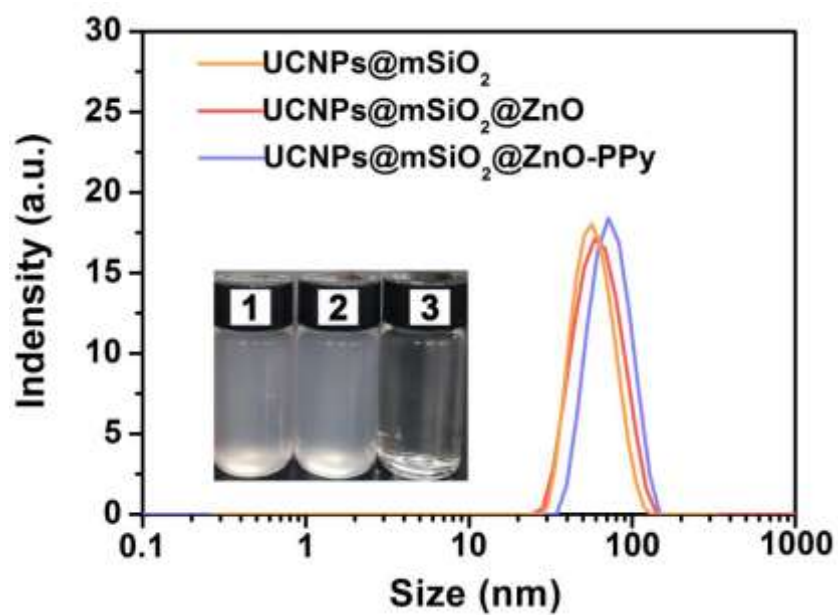


Fig. S4 The dynamic light scattering (DLS) of UCNPs@mSiO₂, UCNPs@mSiO₂@ZnO, and UCNPs@mSiO₂@ZnO-PPy. (inset: the representative photographs of (1) UCNPs@mSiO₂, (2) UCNPs@mSiO₂@ZnO and (3) UCNPs@mSiO₂@ZnO-PPy solutions).

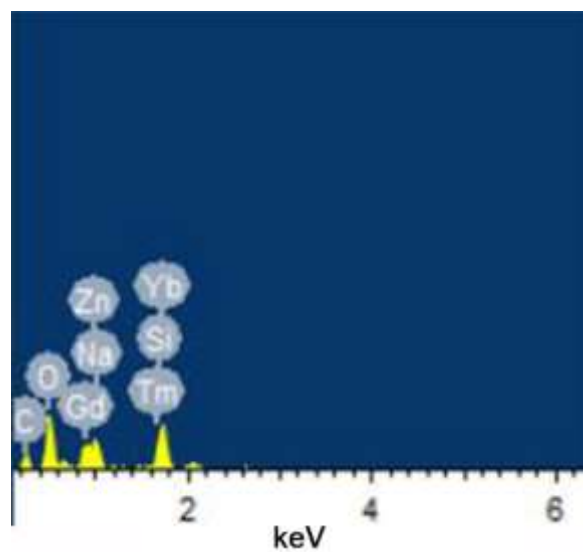


Fig. S5 EDS spectrum of UCNPs@mSiO₂@ZnO.

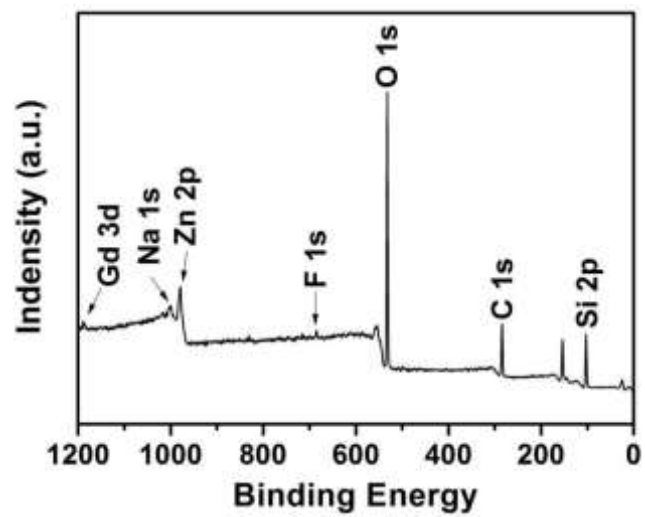


Fig. S6 XPS spectrum of UCNPs@mSiO₂@ZnO.

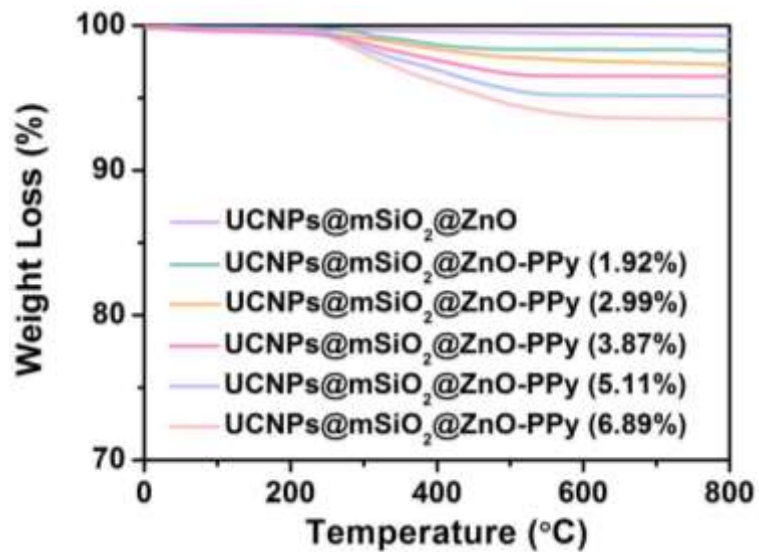


Fig. S7 TGA curves of UCNPs@mSiO₂@ZnO-PPy obtained with different coating amount of PPy.

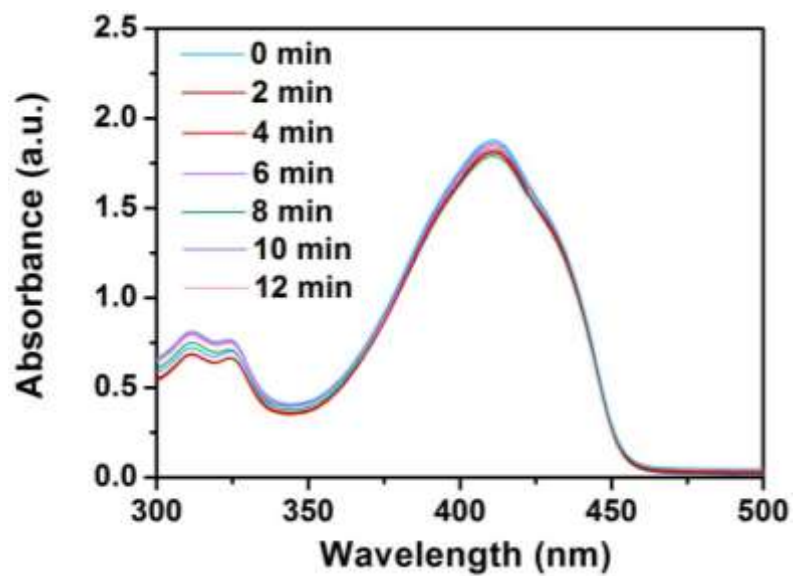


Fig. S8 The variation trend of the absorbance of DPBF solutions without UCNPs@mSiO₂@ZnO-PPy.

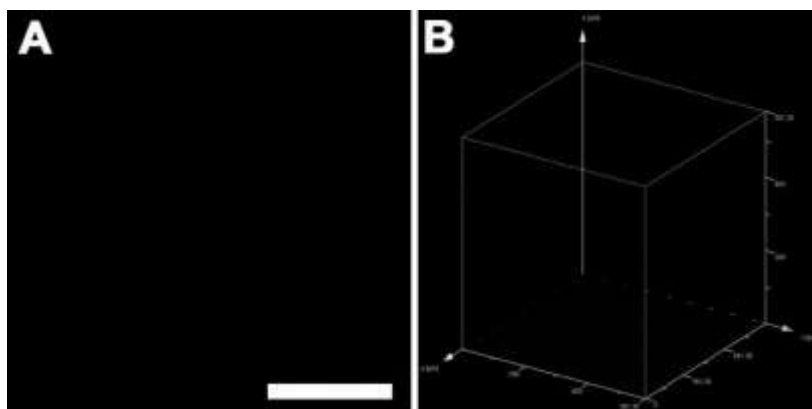


Fig. S9 (A) Intracellular ROS generation detected in HeLa cells treated with DCFH-DA under 980 nm light irradiation. Scale bar is 50 μm . (B) Fluorescence intensity of HeLa cells with 980 nm NIR light irradiation dealt with DCFH-DA for 9 min.

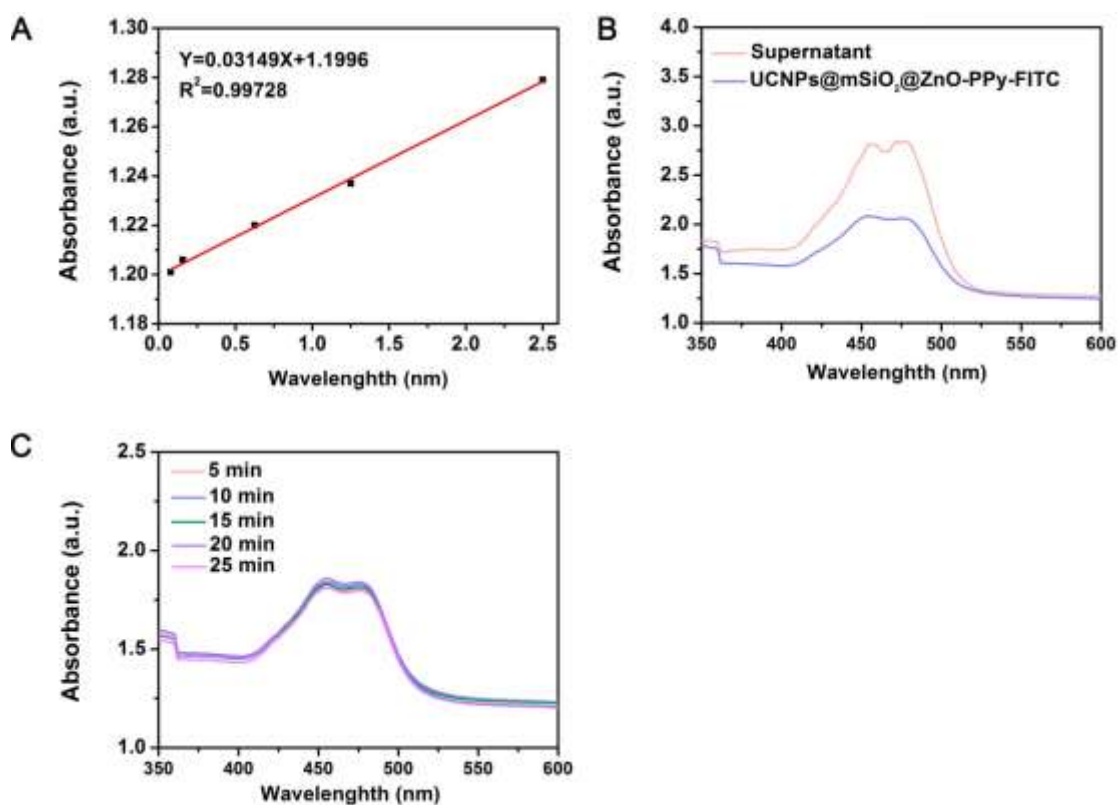


Fig. S10 (A) The standard curve for FITC. (B) The initial UCNPs@mSiO₂@ZnO-PPy-FITC solution and the supernatant obtained after the FITC coating process with UCNPs@mSiO₂@ZnO-PPy. (C) Variation in UV-vis absorption spectra of the UCNPs@mSiO₂@ZnO-PPy-FITC solution after coating for 5, 10, 15, 20 and 25 min.

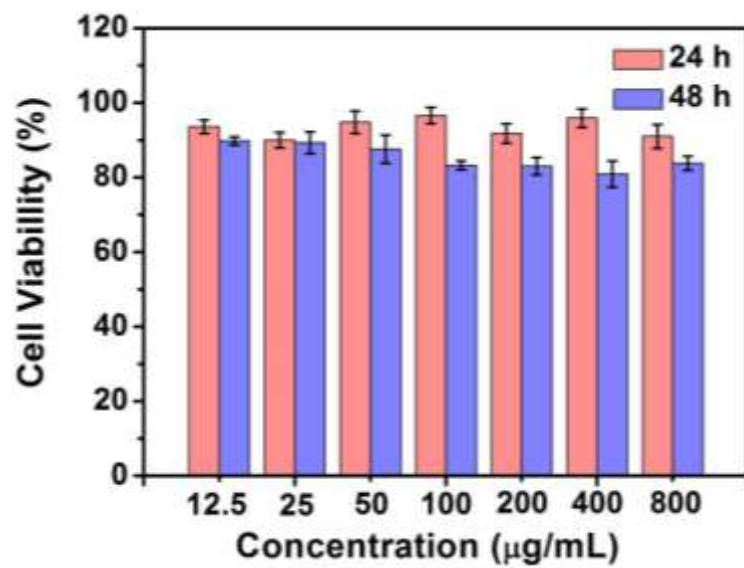


Fig. S11 Quantitative assay of cell viabilities incubated with UZNPs-PPy NPs by standard MTT proliferation test versus incubation concentration for 24 h and 48 h.

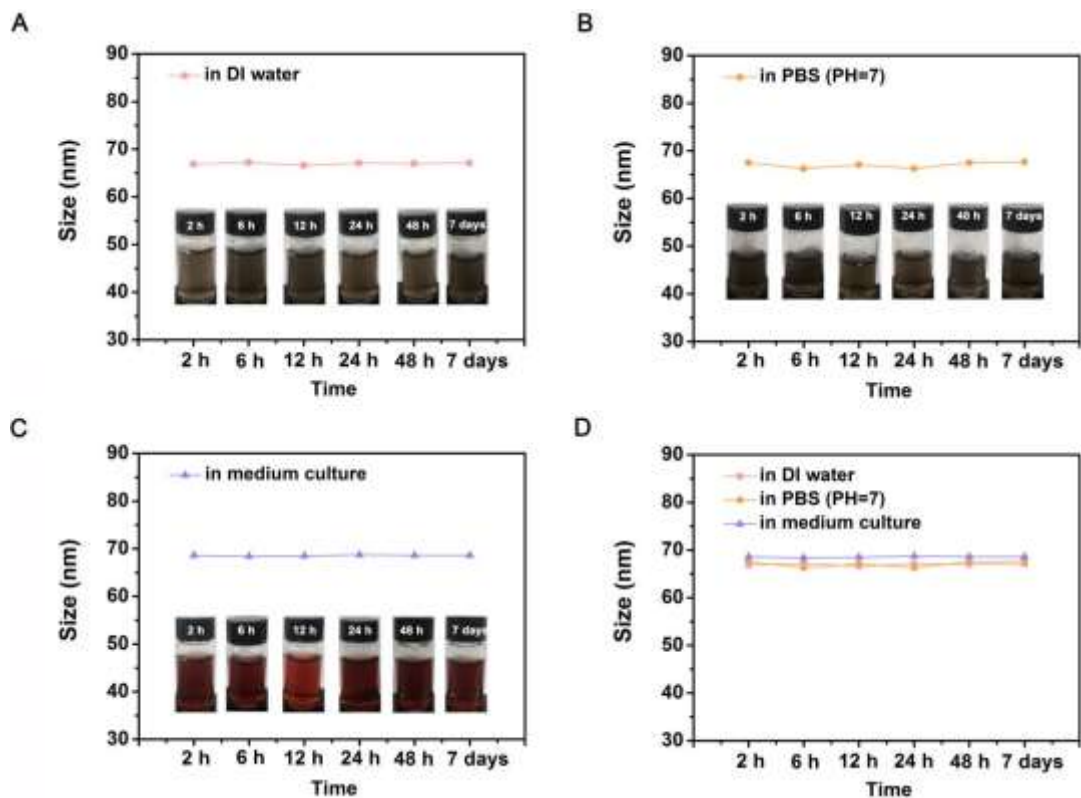


Fig. S12 Variation of size distribution of UCNPs@mSiO₂@ZnO-PPy in (A) H₂O, (B) PBS and (C) culture medium for different times (insets are the corresponding digital photographs). (D) Variation of size distributions of irradiated UCNPs@mSiO₂@ZnO-PPy in different solutions.

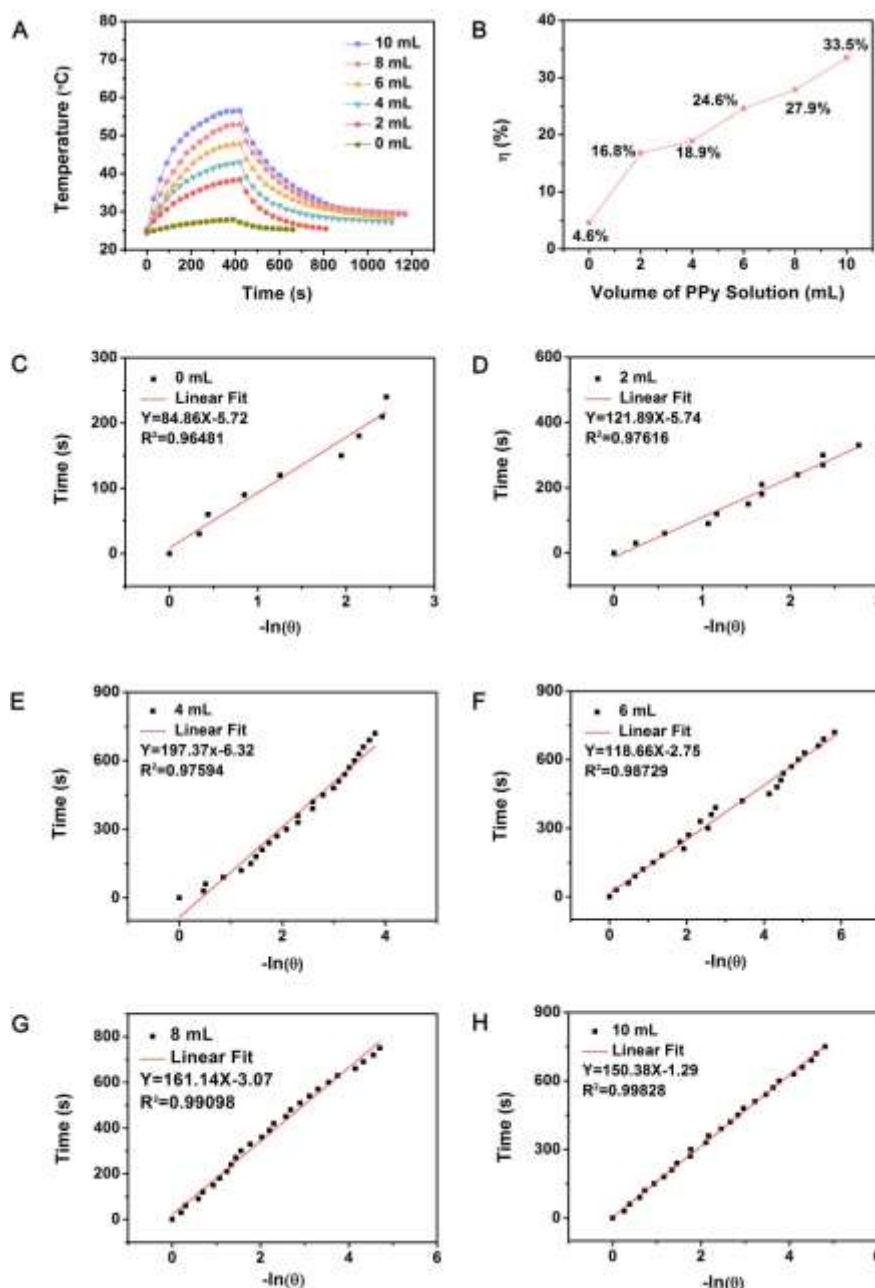


Fig. S13 (A) Temperature change curves of UZNPs-PPy coating with different concentrations of PPy solutions under 980 nm NIR light irradiation. (B) Photothermal conversion efficiency (η) of UZNPs-PPy coating with different concentrations of PPy under 0.5 W cm^{-2} 980 nm laser for 7 min. Linear time data versus $-\ln\theta$ obtained from the cooling period of panel A (C: 0 mL; D: 2 mL; E: 4 mL; F: 6 mL; G: 8 mL; H: 10 mL of $\text{FeCl}_3 \cdot 6\text{H}_2\text{O}$ solution (6 mg mL^{-1})).

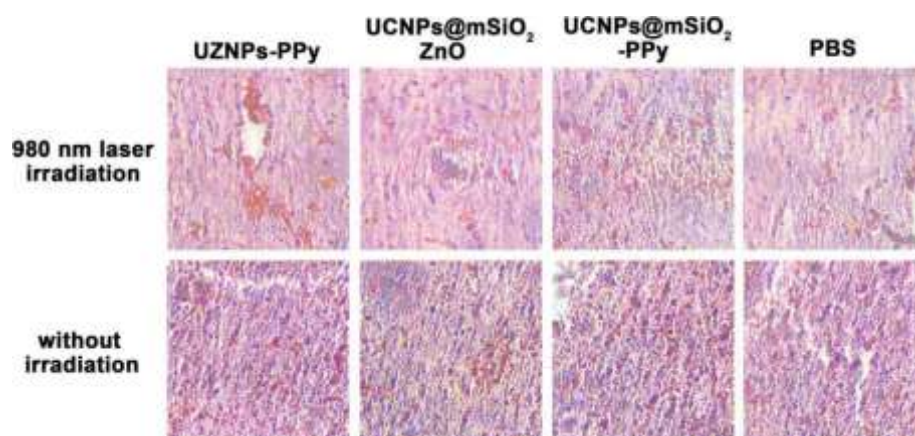


Fig. S14 H&E stained images of tumor tissues obtained after 14 days of treatment.

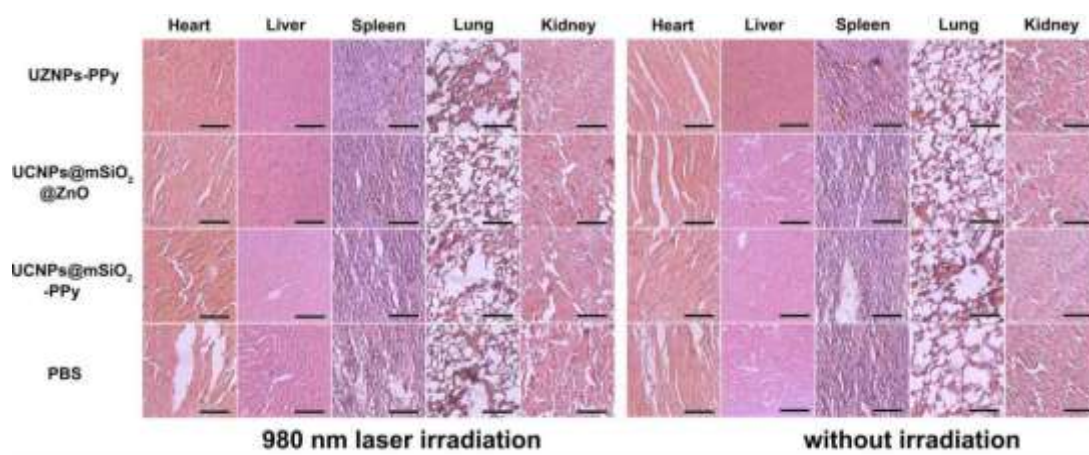


Fig. S15 The hematoxylin and eosin stained images of major organs after treatment for 14 days with and without 980 nm laser irradiation (0.5 W cm^{-2} , 5 min). All images share the same scale bar of $50 \mu\text{m}$.

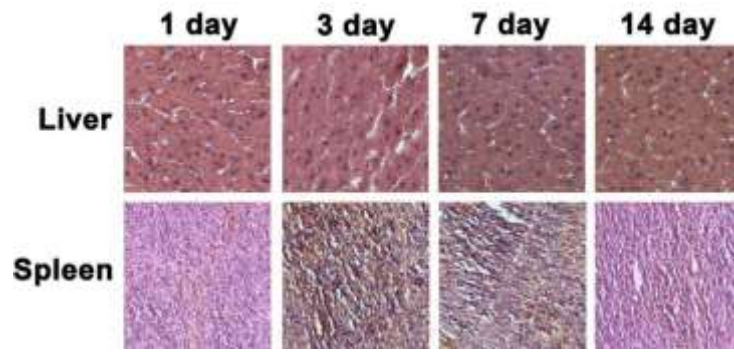


Fig. S16 H&E images of the kidneys and livers of the mice with different times.

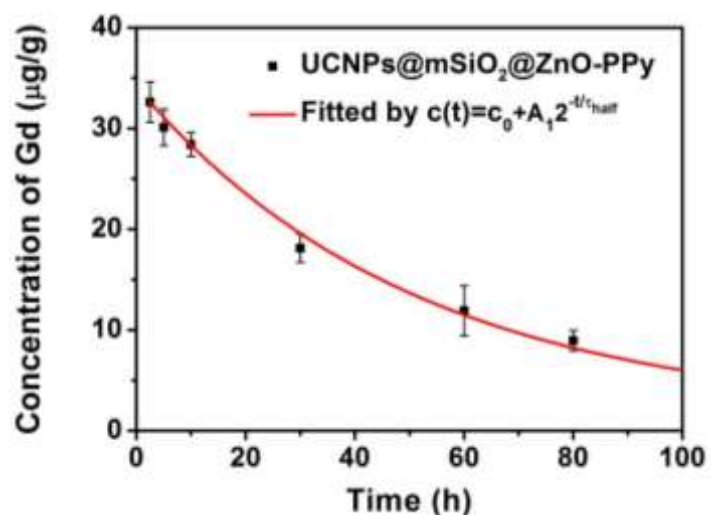


Fig. S17 The blood circulation time in U14 mice after intravenous injection of UCNPs@mSiO₂@ZnO-PPy. Error bars indicate standard deviations, N = 5. $c(t)$ is the intensity at time t (min), c_0 is the intensity at $t = 0$, and τ_{half} is the circulation half-life of the UCNPs@mSiO₂@ZnO-PPy.

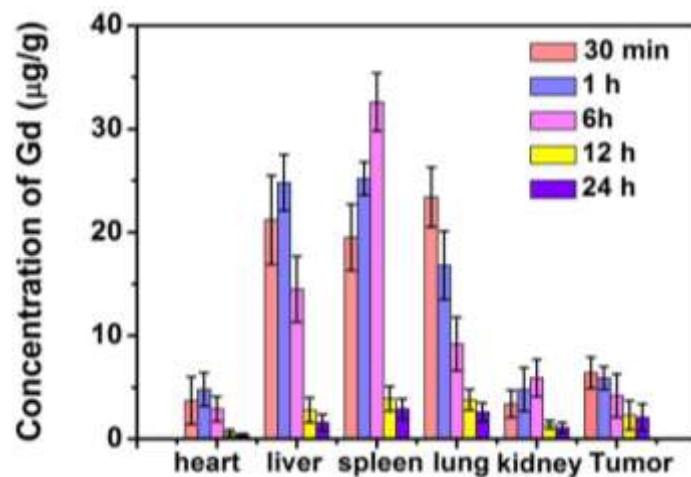


Fig. S18 The bio-distribution of Gd in major organs of mice after injection of UCNPs@mSiO₂@ZnO-PPy intravenously at different time points. Error bars indicate standard deviations, N = 5.